Wireless Power Transfer, 2018, 5(1), 1–8. © Cambridge University Press, 2017
doi:10.1017/wpt.2017.17

RESEARCH ARTICLE

Wireless power transfer (WPT) system for an electric vehicle (EV): how to shield the car from the magnetic field generated by two planar coils

TOMMASO CAMPI[1], SILVANO CRUCIANI[1], VALERIO DE SANTIS[1], FRANCESCA MARADEI[2] AND MAURO FELIZIANI[1]

This paper deals with the shielding of the magnetic field generated by two planar coils of a wireless power transfer (WPT) system at the frequency of tens of kilohertz used in automotive applications. Different shielding techniques using conductive and magnetic materials are examined and discussed highlighting strong and weak points of each other. Finally, the proposed shielding configuration consisting of a combined conductive and magnetic material is applied to model an electric vehicle equipped with a WPT charging system. With this configuration, compliance with the electromagnetic field safety standards can be achieved inside (passengers) or near (pedestrian) the car.

Keywords: Wireless power transfer, electric vehicle (EV), magnetic field, inductive coupling

Received 20 July 2017; Revised 27 September 2017; Accepted 21 October 2017; first published online 27 November 2017

I. INTRODUCTION

The wireless power transfer (WPT) based on the magnetic resonant coupling between two or more coils is a very promising technology to transfer electrical energy without wires [1–13]. For this technology to become widespread in the next future, it is necessary that the magnetic field generated in the environment by WPT systems must be compliant with:

- electric and magnetic field (EMF) safety standards for human exposure [14];
- electromagnetic compatibility (EMC) regulations to avoid disturbances with other electric and electronic apparatuses and devices [15].

The compliance with the EMF and EMC regulations is very important, especially for the applications that require high power transfer rate [16], such as inductive charging for electric vehicles (EVs), where the transferred power can be up to 22 kW [17]. For the aforementioned reasons, the mitigation of the magnetic field is of paramount importance.

Current regulation for automotive WPT systems imposes the operational frequency of 85 kHz [17]. At this frequency, the magnetic field reduction in the environment can mainly be obtained in two ways: by (passive) shielding techniques using conductive and/or magnetic material panels or adding one or more (active) coils [18–20]. However, the WPT system is an intentional source of magnetic field. Thus, any field reduction using improperly active or passive shields could dramatically reduce the performances of the WPT itself that becomes unable to transfer the nominal power to the load [1, 2].

Several studies aimed to mitigate the magnetic field emitted by two planar coils for WPT applications have already been proposed. In [11], some passive magnetic shield configurations have been compared to find the best solution in terms of coupling factor between the coils. In a previous study from the authors [12], an optimization procedure of the magnetic shield has been proposed to reduce the emitted magnetic field, while in [13] a detailed study of the shielding techniques through active coils has been carried out. However, all these studies have focused their attention either on the WPT efficiency or on the magnetic field reduction.

In this study, both the reduction of the magnetic field in the desired zone and the influence of the shield on the electrical performances are taken into account. Those aspects are very important in automotive applications, where the magnetic field must be reduced without an excessive degradation of the system performances. To achieve these results, a passive shielding technique made by a combination of conductive and magnetic material panels has been investigated.

The considered WPT system is composed of two parallel coupled coils: the primary placed outside the EV on the road, while the secondary is located in the vehicle underbody

[1]Department of Industrial and Information Engineering and Economics, University of L'Aquila, L'Aquila, Italy
[2]Department of Astronautics, Electrical and Energetic Engineering, Sapienza University of Roma, Roma, Italy
Corresponding author:
T. Campi
Email: tommaso.campi8888@gmail.com

in close proximity of many metallic objects as chassis, platform, engine, electrical wiring system, etc. The coupled coils are modeled by an equivalent two-port network whose circuit lumped parameters are depending not only on the configurations of the coils but also on the conductive and magnetic materials in the surrounding environment [1, 2].

The magnetic field and the influence of the shields on the WPT efficiency are validated by measurements carried out in a simple WPT system demonstrator. Finally, several shield configurations using both magnetic and conductive material panels are proposed considering a real automotive WPT system. In this case, the presence of the conductive chassis of the vehicle is taken into account in order to find the best solution to mitigate the magnetic field created by the same WPT system while maintaining high efficiency. The obtained magnetic field levels for the optimized solution are then compared with EMF safety limits, i.e., the reference level (RL), provided by the ICNIRP guidelines [14]. Some discussions on the magnetic shielding in future EVs made of carbon-fiber panels are also outlined.

II. WPT SYSTEM SHIELDING

A) Conductive shielding

Shielding of magnetic near fields is a relevant problem for EMC engineers. It is well known that the use of metallic panels can be inadequate to mitigate the magnetic field at very low frequencies [1, 2]. The magnetic shielding effectiveness (SE_H) for a time-harmonic field is defined as:

$$SE_H = 20\log_{10}(H^i/H), \tag{1}$$

where H and H^i are the magnetic fields at the observation point in the presence and in absence of the shield, respectively.

Considering a one-dimensional problem as a plane wave impinging normally on an infinite shield panel, SE_H for conductive shields can be approximated by [20]

$$SE_H = A_{dB}(\omega) + R_{dB}(\omega) + M_{dB}(\omega), \tag{2}$$

where ω is the angular frequency, A_{dB} represents the absorption loss of the wave as it proceeds through the shield barrier, R_{dB} represents the reflection loss caused by the field reflection on the shield surface, and M_{dB} represents the additional effects of multiple reflections and transmissions.

For magnetic near field sources, the most significant term in (2) is the absorption loss $A_{dB} = 20\log_{10}(e^{t/\delta})$, t being the shield thickness and $\delta = (\pi f\mu\sigma)^{-1/2}$ the skin depth shown in Fig. 1 for copper and aluminum shields. The shielding performances of copper and aluminum are good enough (e.g., $\delta \approx 0.25$ mm at $f = 85$ kHz), but there is another relevant problem due to the eddy currents induced in the conductive shield producing a magnetic field opposite to the incident one. As a consequence, the inductive coupling between coils is reduced as well as the WPT performances. A further problem is given by the strong detuning of the WPT system due to the decrease of the inductances. Thus, the resonance condition can be obtained again at the nominal frequency only by varying the compensation capacitors [1, 2].

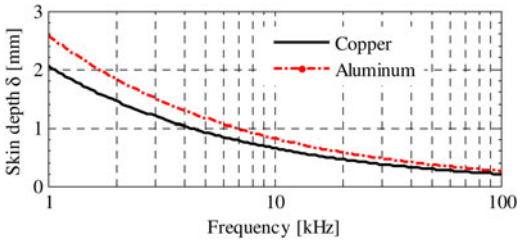

Fig. 1. Penetration depth in conductive materials (copper and aluminum).

B) Magnetic shielding

The magnetic shielding consists of using high magnetic permeability material panels that provide a preferential path for the magnetic flux lines. The incident magnetic field is not "blocked" as in conductive shields, but it is diverted into the magnetic material. The use of magnetic panels improves the quality of the WPT system for two separate reasons:

(1) the magnetic coupling between the primary and the secondary coil increases due to the presence of magnetic materials that can be assumed to be a portion of a magnetic core;
(2) the magnetic flux lines following the path of minimum reluctance are diverted from the region to be shielded into the magnetic materials producing a shielding effect.

The magnetic shielding effectiveness using magnetic shields is difficult to be evaluated by formulas since it mainly depends on the magnetic field configuration. However, at the frequency of interest, the use of low loss, high resistivity magnetic materials, such as ferrites, is highly recommended.

III. EQUIVALENT CIRCUIT

A) Equivalent circuit of a WPT system

A WPT coil system without compensation can be modeled as a two-port network characterized by a 2×2 chain matrix Φ, as shown in Fig. 2(a). This network can be modeled by a T-type circuit (see Fig. 2(b)) with frequency-dependent impedances Z_1, Z_{12}, and Z_2 that depend on the WPT coil configuration. The relationships among Z_1, Z_{12}, Z_2 and the chain matrix coefficients Φ_{11}, Φ_{12}, Φ_{21}, and Φ_{22} are given by

$$Z_1 = (\Phi_{11} - 1)/\Phi_{21}, \tag{3a}$$

$$Z_2 = (\Phi_{22} - 1)/\Phi_{21}, \tag{3b}$$

$$Z_{12} = 1/\Phi_{21}. \tag{3c}$$

To improve the WPT system performances, the primary and secondary coils are compensated introducing series or parallel capacitors to obtain the resonance condition [9]. Considering series–series (SS) primary and secondary compensation blocks characterized by 2×2 chain matrices Φ_{c1}

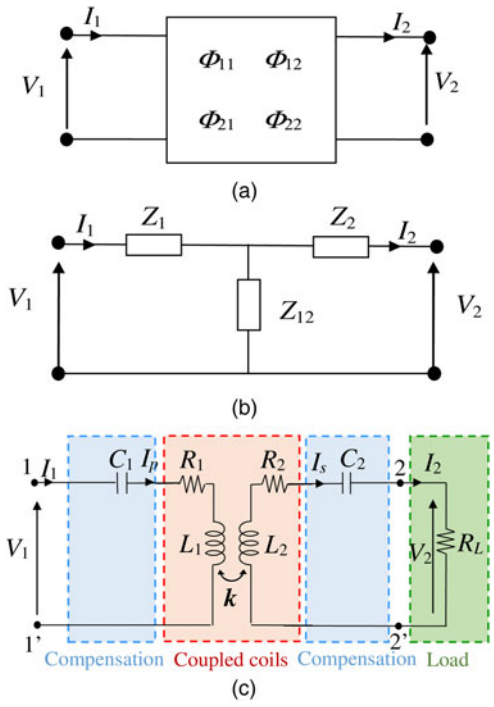

Fig. 2. The equivalent circuit of a WPT coil system modeled by a two-port network (a). T-type circuit with lumped impedances (b). SS configuration with load resistance R_L (c).

and Φ_{c2}, respectively, the total chain matrix of the circuit in Fig. 2(c) is given by $\Phi_t = \Phi_{c1}\Phi\,\Phi_{c2}$.

The WPT efficiency is defined as

$$\eta = P_2/P_1, \tag{4}$$

where P_2 is the real power transferred to the load Z_L and P_1 is the real power at the input port of the primary circuit, respectively. The efficiency can also be expressed as

$$\eta = \frac{Re(Z_L)|I_2|^2}{Re(Z_{in})|I_1|^2}, \tag{5}$$

where Re is the real part operator, I_1 is the primary current at the port 1–1′, I_2 is the secondary current at the port 2–2′, and Z_{in} is the input impedance at the port 1–1′ given by

$$Z_{in} = \frac{\Phi_{t,11}Z_L + \Phi_{t,12}}{\Phi_{t,21}Z_L + \Phi_{t,22}}. \tag{6}$$

In the equivalent circuit V_1 and V_2 are the port voltages, while I_p and I_s are the currents flowing into the coils. It should be noted that $I_1 = I_p$ and $I_2 = I_s$ for the SS compensation topology.

Applying (6) in (5), the WPT efficiency can be rewritten as:

$$\eta = \frac{R_L}{Re((\Phi_{t,11}R_L + \Phi_{t,12})conj(\Phi_{t,21}R_L + \Phi_{t,22}))}, \tag{7}$$

where *conj* represents the conjugate of a complex quantity and when the load impedance $Z_L = R_L$ is purely resistive.

B) Coils in air

Two coils in the air can be modeled by the previously described equivalent circuits whose impedances are given by [2]

$$Z_1 = R_1 + j\omega(L_1 - M), \tag{8a}$$

$$Z_2 = R_2 + j\omega(L_2 - M), \tag{8b}$$

$$Z_{12} = R_{12} + j\omega M, \tag{8c}$$

where $R_1 = R_1(\omega)$ and $R_2 = R_2(\omega)$ are the coil resistances, $L_1 = L_1(\omega)$ and $L_2 = L_2(\omega)$ are the coil self-inductances, $R_{12} = R_{12}(\omega)$ is the mutual resistance, if any, and $M = k(L_1L_2)^{1/2}$ is the mutual inductance, k being the coupling factor. The frequency dependence of the circuit parameters is due to the skin effect in the conductors. Compensation capacitors are added to the WPT system to obtain the resonance and improve the performances. For a SS configuration, the compensation capacitors at the resonant angular frequency ω_o are given by [6]

$$C_1 = 1/(\omega_o^2 L_1), \tag{9a}$$

$$C_1 = 1/(\omega_o^2 L_2), \tag{9b}$$

and the efficiency η in the resonance condition and for a resistive load R_L is given by

$$\eta = \frac{R_L(R_{12}^2 + \omega_o^2 M^2)}{(R_{12} + R_2 + R_L)^2\left(R_1 + \dfrac{(R_2 + R_L)R_{12} + \omega_o^2 M^2}{R_{12} + R_2 + R_L}\right)}. \tag{10}$$

The efficiency η increases as ω_o and k increase and as R_1, R_2, and R_{12} decrease. Furthermore, the efficiency depends strongly on the load resistance R_L [5]. A similar behavior is observed for different capacitance compensation topologies, such as series-parallel (SP), parallel-series (PS), and parallel-parallel (PS) configurations [6].

C) Coils in the presence of lossy conductive materials

The equivalent circuit of a WPT system in the presence of lossy conductive materials in the surrounding has the same topology as described above, but with different values of lumped circuit parameters. Using the prime ′ symbol for this new configuration, it yields that $R_1' \geq R_1, R_2' \geq R_2, R_{12}' \geq R_{12}, L_1' \leq L_1, L_2' \leq L_2, k' \leq k$, $M' \leq M$. The coupling factor k is reduced because the time-varying magnetic field generated by the WPT system induces eddy currents on the conductive shield. Thus, these currents generate a magnetic field opposite to the incident one reducing the self-inductance of the coils and consequently the coupling factor.

D) Coils in the presence of magnetic lossless materials

Since the AC losses can be negligible in some magnetic materials with very low conductivity, i.e., ferrite, the equivalent circuit of a WPT in the presence of lossless magnetic materials in the

surrounding is again the same. However, some circuit parameters are different from those with coils in the air due to the presence of the magnetic material that modifies the magnetic field behavior [1]. Using the asterisk * symbol for this configuration it yields: $R_1^* \approx R_1$; $R_2^* \approx R_2$; $R_{12}^* \approx R_{12}$; $L_1^* \geq L_1$; $L_2^* \geq L_2$; $k^* \geq k$; $M^* \geq M$. At the resonant frequency the efficiency increases, $\eta^* \geq \eta$, due to the increase of k^*. This favorable behavior can be physically explained by the presence of the magnetic material that can be considered as a portion of a magnetic core improving the magnetic coupling (described by the increase of k^*) and reducing the magnetic flux leakage. If the magnetic shield is lossy, the behavior can be described by a combination of the previous equations for conductive and lossless magnetic materials. In this case, it is quite impossible to know *a priori* if the efficiency increases or decreases

IV. METHOD VALIDATION

In order to validate the numerical results and experimentally evaluate the shielding performances of simple shielding panels, a WPT demonstrator has been realized, as shown in Fig. 3(a). The primary coil is fed by an inverter that generates a square wave voltage source V_s at the nominal frequency $f_o = 85$ kHz. The value of *versus* is regulated using a DC/DC converter before the inverter (see the picture in Fig. 3(b)) in order to transfer a fixed power $P_2 = 100$ W to a resistive load $R_L = 5\ \Omega$.

Three test cases are examined:

- coils in the air without a shield;
- coils in the presence of an aluminum conductive shield placed near the secondary coil;
- coils in the presence of a ferrite magnetic shield placed near the secondary coil.

As shown in Fig. 4, the shielding panels of conductive or magnetic material have side length $l_s = 15$ cm and different thickness t. The WPT demonstrator has two identical coaxial planar coils with $N_1 = N_2 = 5$ turns, internal coil radius $R_{int} = 70$ mm, external coil radius $R_{ext} = 83.5$ mm, enameled copper wire with diameter $D = 2.5$ mm, and the distance between the stacked coils $d_c = 40$ mm. The panels under test are placed parallel to the secondary coil at a distance $d_s = 3$ mm, and their characteristics are reported in Table 1.

First, the equivalent circuit parameters of the WPT coil system are extracted by a numerical software tool based on the finite element method (FEM) [6], as reported in Table 2. The equivalent circuit analysis is then used to evaluate the efficiency η, the real power P_1 and the primary coil currents I_p, when the load power $P_2 = 100$ W and $I_2 = I_s = 4.4$ A are fixed. The measured values are compared with those obtained by the circuit analysis as reported in Table 3. The output power P_2 in both calculations and measurements is kept fixed by adjusting the input voltage V_1 of the source block.

It should be noted that the presence of a conductive shield leads to a reduction of k and therefore of the WPT performance, while the presence of a low loss magnetic shield leads to an increase of k and therefore of the WPT performance.

Finally, the magnetic flux density vector $\boldsymbol{B}$ is evaluated by a FEM electromagnetic field solver assuming as magnetic field sources the coil currents I_p and I_s derived from the circuit analysis [12]. The rms magnitude $|\boldsymbol{B}|$ of the magnetic flux density is calculated and measured at a distance $d_M = 8$ cm above the secondary coil for the three test cases, as shown in Fig. 5,

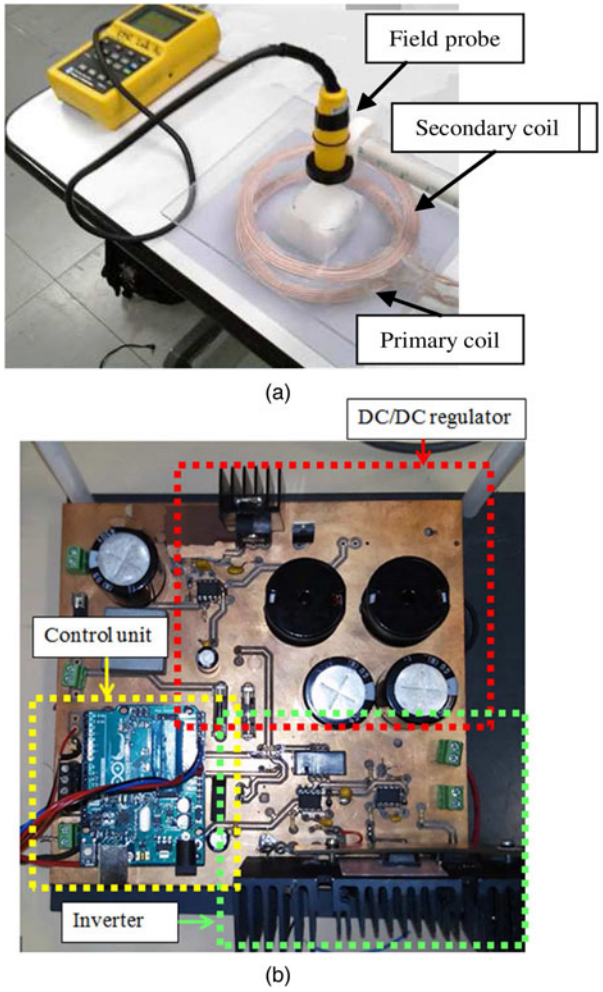

Fig. 3. WPT demonstrator. (a) Measurement setup. (b) Realized inverter with DC/DC regulator.

where a good agreement is observed. From the obtained results we draw the following conclusions: the presence of a conductive panel provides excellent shielding performance but the WPT efficiency is drastically reduced, while a magnetic shield could lead to both a good shielding and high efficiency of the WPT system when it is adequately designed.

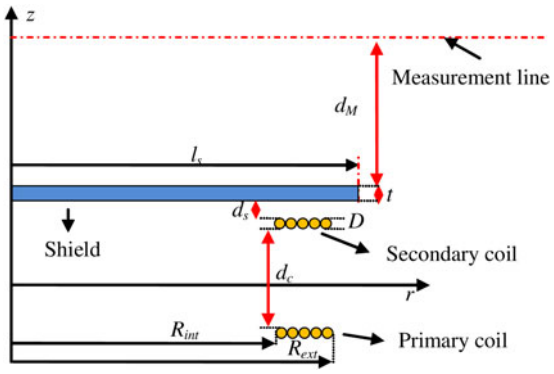

Fig. 4. 2D axially-symmetric configuration of a two-coil system in presence of a shielding panel used for the method validation.

Table 1. Shield configurations at 85 kHz.

Test case	Material	σ (S/m)	μ_r	t (mm)	Skin depth δ (mm)
1	Aluminum	3.7×10^7	1	1	0.28
2	Ferrite	10	2400	4	11

Table 2. Measured and calculated inductances at 85 kHz.

Test case	Calculated			Measured		
	L_1 (μH)	L_2 (μH)	M (μH)	L_1 (μH)	L_2 (μH)	M (μH)
No shield	7.43	7.43	2.02	7.23	7.47	2.32
Conductive shield	6.73	2.41	0.41	6.39	2.31	0.35
Magnetic shield	7.68	11.27	3.02	7.79	11.44	3.35

Table 3. Measured and calculated electrical quantities.

Test case	Calculated			Measured		
	P_1 (W)	η (%)	I_p (A)	P_1 (W)	η (%)	I_p (A)
No shield	110	90	20.8	115	87	19.5
Conductive shield	181	55	59.2	188	52	57.2
Magnetic shield	105	95	13.9	107	93	14.2

V. AUTOMOTIVE APPLICATIONS

A realistic automotive WPT application is also examined. The considered WPT system is designed and optimized to efficiently transfer a power of 7.7 kW to the load which models the battery charger of a mid-size car. The WPT system operates at 85 kHz and has two identical circular planar coils, with external diameter $R_{out} = 250$ mm and number of turns $N_1 = N_2 = 10$. The distance between the stacked coils is $d_c = 200$ mm. The coils are made of Litz wire to reduce the AC losses at the considered frequency [21]. The Litz wire is composed of 1050 strands of AWG 38 copper wire with a geometrical diameter of about $D = 6$ mm. The load is modeled as a simple power resistor $R_L = 10\ \Omega$. The SS compensation topology is adopted and the WPT system is fed by a time-harmonic voltage generator source V_s [21, 22]. Due to the geometrical complexity, the AC resistance of the Litz wire coils is not calculated but obtained from datasheets. Their values are $R_1 = R_2 = 94\ \text{m}\Omega$ at the frequency of 85 kHz.

Several shielding configurations assuming conductive shields, magnetic shields, or a combination of conductive and magnetic shields are considered, as shown in Fig. 6. The shield configurations of the primary and secondary coils are identical. The examined new test case configurations are:

#0: no shield (i.e., coils in the air);
#1: conductive shield;
#2–3: magnetic shields;
#4–5–6: combinations of magnetic and conductive shields.

In the test cases, #1, #4, #5, and #6 the conductive shield is made by an aluminum disk with radius $R_{al} = 500$ mm, thickness $t = 2$ mm, $\mu_r = 1$, and $\sigma = 37$ MS/m. The material used

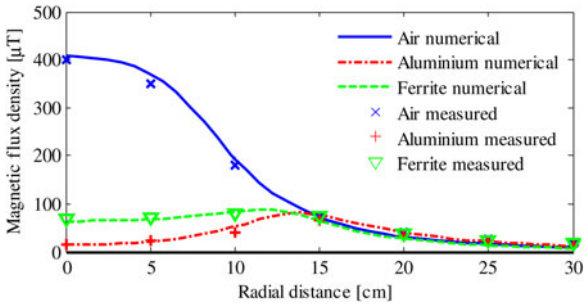

Fig. 5. Magnetic flux density $|\boldsymbol{B}|$ along the r-axis at $z = d_M + t + d_s + D + d_c/2$.

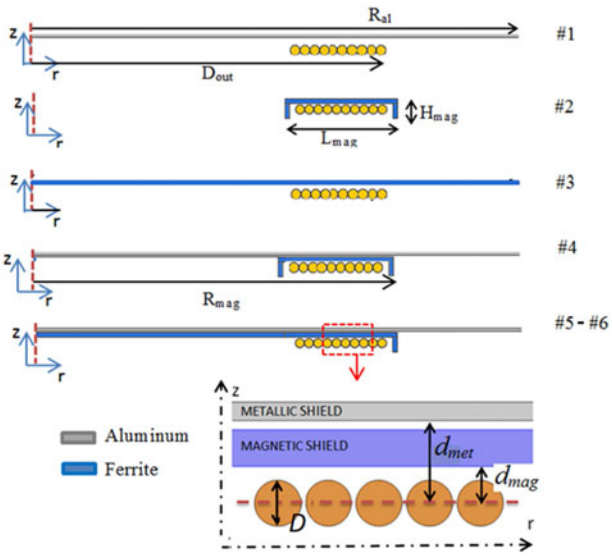

Fig. 6. 2D axially-symmetric shield configuration for test cases #1–6 (only the secondary coil is depicted since the primary coil is specular).

for all magnetic shields is a ferrite of different shape and dimension but always characterized by a relative permeability $\mu_r = 2400$ and conductivity $\sigma = 10$ S/m.

The ferrite shield thickness is $t = 4$ mm for all test cases except for case #3, where a thicker shield of $t = 6$ mm is considered. In the test cases, #2 and #4 the magnetic shields are shaped as a circular corona with a C-shaped cross-section having dimensions $L_{mag} = 100$ mm and $H_{mag} = 30$ mm. In the test cases, #5 and #6 the magnetic shield is a disk with the L-shaped section, while in test case #3 the magnetic shield is a simple disk with radius $R_{mag} = 500$ mm. The distance between the magnetic shields and the coil is $d_{mag} = 5$ mm. The distance from the conductive shield to the coil is $d_{met} = 11$ mm for all cases, except for test case #6 where the distance is set to $d_{met} = 22$ mm. Cases #5 and #6 are presented to verify the influence of the parameter d_{met} on the efficiency and on the magnetic field.

The lumped circuit parameters and the WPT performance quantities (i.e., self-inductance $L_1 = L_2 = L$, mutual inductance M, efficiency η, input voltage V_1, and current I_1) are calculated following the method described in the previous section. Table 4 summarizes the obtained results of all the considered test cases. It should be noted that for each test case the values of the compensation capacitor has been updated to reach the resonant condition at 85 kHz by (9).

The SE_H in WPT systems is not clearly defined since the introduction of a conductive shield affects the inductive

Table 4. Circuit lumped parameters and electrical performances.

Test case	L (μH)	M (μH)	η (%)	I_p (A)	V_1 (V)	k
#0	95.5	18.6	97.9	28.1	278	0.195
#1	15	0.13	0.04	4000	405	0.008
#2	151	30.1	98.5	17.4	447	0.199
#3	189	63	99	9.1	946	0.33
#4	79	11.8	96	44.4	180	0.149
#5	134	19.1	97.2	27.4	285	0.142
#6	138	21.5	98.0	24.0	325	0.155

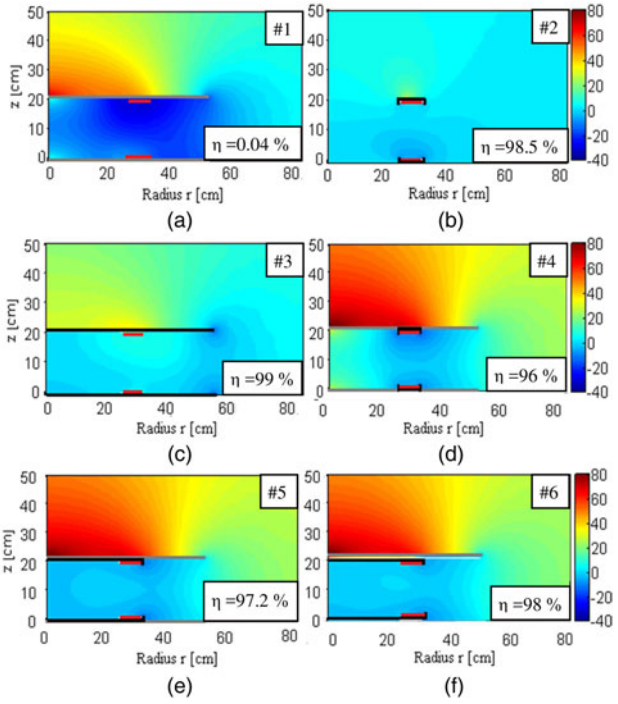

Fig. 7. Maps of shielding effectiveness SE_H for test cases #1 (a), #2 (b), #3 (c), #4 (d), #5 (e), and #6 (f).

coupling modifying the incident field H^i [1, 2]. In this work, the calculation of SE_H is performed keeping constant the output quantities P_2, V_2, and I_2. The primary voltage V_1 is adjusted for each test case in order to keep fixed the power level delivered to the load at $P_2 = 7.7$ kW. The output voltage is $V_2 = 277$ V, while the output current is $I_2 = 28$ A.

The magnetic shielding effectiveness SE_H is then calculated at any point by (1) using an eddy current solver. The maps of the shielding effectiveness for all test cases are shown in Fig. 7, when considering H^i the field produced by the WPT coil currents in absence of shielding (i.e., in air) when $P_2 = 7.7$ kW and $I_2 = 28$ A. In the test case #1 (only large conductive shield simulating the vehicle chassis) the SE_H is significant but, as described above, the WPT efficiency is very low and makes the system useless. In the test case #2 and #3 (only magnetic material), the shielding effect is poor in the case #2 while in the test case #3 where the larger dimension and thickness of the shield leads to good SE_H performances. Furthermore, the use of only magnetic shield permits to optimize the WPT performances with a maximum efficiency of 99% obtained for test case #3. In the other test cases (#4–6), the magnetic and conductive shields are combined placing the magnetic field between the coil and the conductive shield. These configurations produce similar results in terms of shielding effectiveness and WPT efficiency. The small differences between them are mostly due to the different geometrical configuration of the magnetic shield that diverts the magnetic flux lines in a different way. The best compromise in terms of SE_H and η is obtained for the electro-geometrical configurations of test cases #5 and #6. However, the increment of the distance between the metallic shield and the coils (d_{met}) leads to a very small increase in the efficiency, while the SE_H maps are almost identical. Since the increase of d_{met} could lead to mechanical problems, together with space and weight, there is no point to suggest test case #6.

Finally, the magnetic field distribution inside a realistic EV chassis made of aluminum has been calculated considering a shielding configuration similar to the test case #5. In this case, the metallic shield is replaced by the presence of the EV bodyshell [4]. This last is assumed to be of aluminum alloy with conductivity $\sigma = 30$ MS/m and thickness $t = 2$ mm. The car outer dimensions are length $l = 4.3$ m, width $w = 1.7$ m, and height $h = 1.2$ m.

To reproduce the real environment in the simulations and to accurately calculate the currents on the coils, the simplified equivalent circuits of the source and load blocks (see again Fig. 2) are replaced with more realistic electronic blocks, as

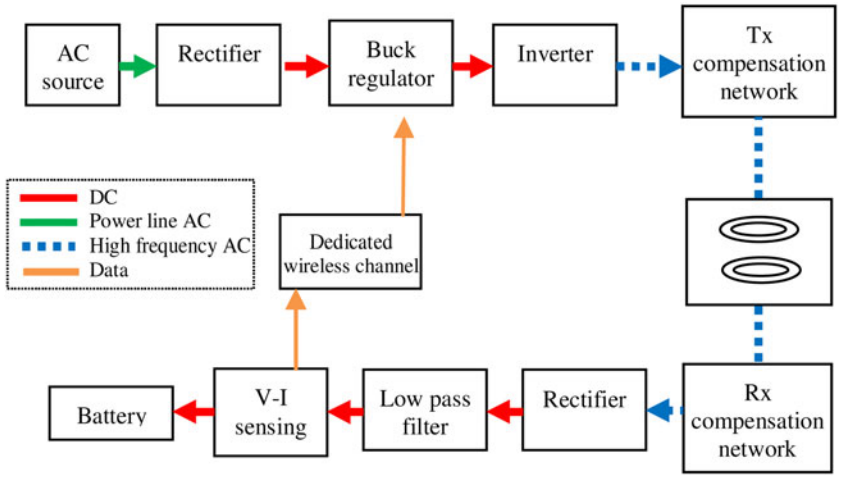

Fig. 8. Block diagram of WPT charger.

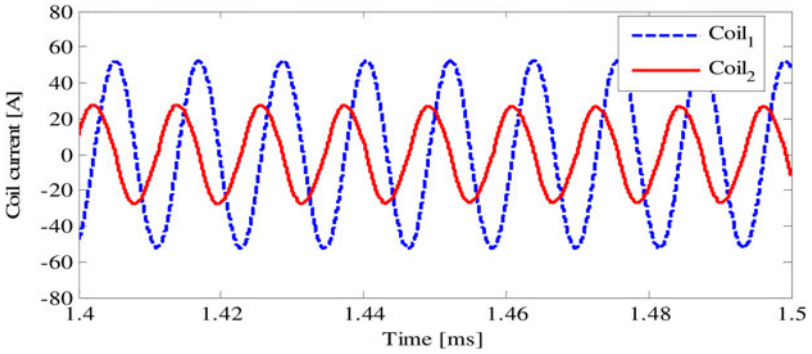

Fig. 9. Waveforms of the currents on the primary and secondary coils.

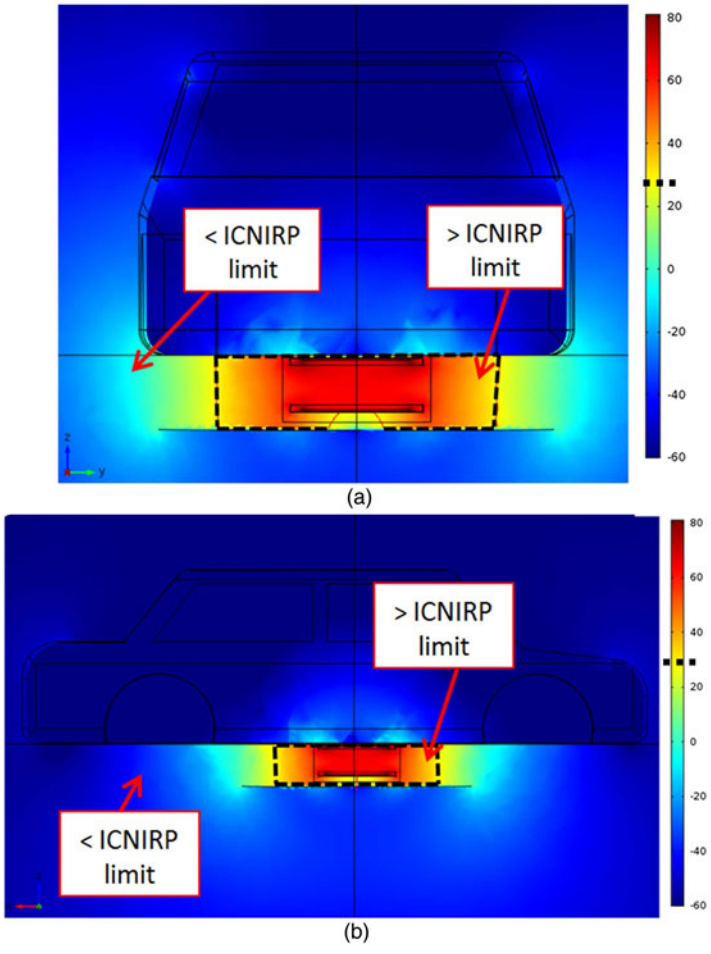

Fig. 10. Magnetic field distribution inside and outside the EV in dBμT. Front view (a). Lateral view (b).

schematically reported in Fig. 8. On the transmitting side, the AC voltage is converted in DC by a rectifier and then a DC/DC converter permits to regulate the feeding voltage of the inverter. This block is used to adjust the output power using an output power feedback given from the battery through a dedicated wireless transmission [23].

The inverter converts the DC voltage into an AC voltage at the resonant frequency f_o. On the receiving side, the high-frequency AC voltage is firstly rectified and then filtered and connected to the battery. In the SPICE simulations, a full bridge inverter with IPW60R045CPA MOSFETs is considered at the transmitting side, while a bridge rectifier (composed of DDB6U145N16L diodes) and a simple LC filter with $L = 0.1$ μH and $C = 100$ μF is applied to the receiving side.

The calculated RMS currents in the primary and secondary coils using SPICE are $I_1 = 22.2$ A and $I_2 = 37.2$ A, and their waveforms are reported in Fig. 9. The magnetic field is then calculated imposing $I_p = I_1$ and $I_s = I_2$ as magnetic field sources in the eddy current solver. The calculated maps of $|\boldsymbol{B}|$ are shown in Fig. 10, where the ICNIRP 2010 reference level ($B_{RL} = 27$ μT ($= 28.63$ dBμT) @ $f = 85$ kHz) are also reported highlighting the zones where the limits are exceeded.

VI. CONCLUSIONS AND DISCUSSIONS

A numerical and experimental analysis has been carried out to evaluate the shielding performances of conductive and magnetic shields excited by two planar coils of a WPT system. Particular attention has been focused on the influence of the shield types and configurations on the electrical performances of the system. The presence of conductive shields generates relevant eddy currents and good shielding performance, but it reduces dramatically the efficiency of the WPT system. On the contrary, the use of a high permeability and low loss material, such as the ferrite, improves the electrical performances of a WPT system. However, to obtain good shielding results, a relevant amount of ferrite could be necessary making the WPT system expensive and cumbersome. The use of a combination of both magnetic and conductive shields permits to maintain high electrical efficiency and excellent shielding performances.

The aforementioned considerations must be kept in mind when considering also the material composition and thickness of the car chassis. For instance, in current EVs made mainly by aluminum alloys, a single magnetic (e.g., ferrite) shield placed under the car platform could be enough to reach reasonable performances. Instead, in future EVs, where the chassis will be made of poor conductive materials, such as carbon fibers composite, the use of only magnetic shields could be impracticable due to the excessive thickness and thus the weight of the same. In this case, a combination of adequate magnetic and conductive shields could be the most affordable solution. Indeed, a very thin (i.e., around 0.3 mm thick equal to the skin depth at these frequencies) aluminum foil would be light but good enough to shield the magnetic field while the ferrite permits to maintain the electrical performances at an acceptable level.

REFERENCES

[1] Cruciani, S.; Feliziani, M.: Mitigation of the magnetic field generated by a wireless power transfer (WPT) system without reducing the WPT efficiency, in *EMC Europe –Int. Symp. on EMC*, Bruges, Belgium, Sept. 2–6, 2013, 610-615.

[2] Campi, T.; Cruciani, S.; Feliziani, M.: Magnetic shielding of wireless power transfer systems, EMC'14, /Tokyo, in *2014 Int. Symp. Electromagnetic Compatibility*, Tokyo, Japan, 2014, 422–425.

[3] Fisher, T.M.; Farley, K.B.; Gao, Y.; Bai, H.; Tse, Z.T.H.: Electric vehicle wireless charging technology: a state-of-the-art review of magnetic coupling systems. Wireless Power Transf., **1** (2) (2014), 87–96.

[4] Campi, T.; Cruciani, S.; De Santis, V.; Maradei, F.; Feliziani, M.: Numerical characterization of the magnetic field in electric vehicles equipped with a WPT system. Wireless Power Transf., (2017), 1–10. Online. Available: https://doi.org/10.1017/wpt.2017.5

[5] Campi, T.; Cruciani, S.; De Santis, V.; Feliziani, M.: EMF safety and thermal aspects in a pacemaker equipped with a wireless power transfer system working at low frequency. IEEE Trans. Microw. Theory Techn., **64** (2) (2016), 375–382.

[6] Campi, T.; Cruciani, S.; De Santis, V.; Palandrani, F.; Hirata, A.; Feliziani, M.: Wireless power transfer charging system for AIMDs and pacemakers. IEEE Trans. Microw. Theory Techn., **64** (2) (2016), 633–642.

[7] Asakura, S.; Kikuma, N.; Hiyayama, H.; Sakakibara, K.: Shielding effect of magnetic resonant wireless power transfer, in *2011 IEICE General Conf.*, Mar. 2011, B 4-69.

[8] Kim, J. et al.; Coil design and shielding methods for a magnetic resonant wireless power transfer system. Proc. IEEE, **101** (6) (2013), 1332–1341.

[9] Wang, C.-S.; Covic, G.A.; Stielau, O.H.: Power transfer capability and bifurcation phenomena of loosely coupled inductive power transfer systems. IEEE Trans. Ind. Electron., **51** (1) (2004), 148–157.

[10] Huh, J.; Lee, S.W.; Lee, W.Y.; Cho, G.H.; Rim, C.T.: Narrow-width inductive power transfer system for online electrical vehicles. IEEE Trans. Power Electron., **26** (12) (2011), 3666–3679.

[11] Budhia, M.; Covic, G.A.; Boys, J.T.: Design and optimization of circular magnetic structures for lumped inductive power transfer systems. IEEE Trans. Power Electron., **26** (11) (2011), 3096–3108.

[12] Campi, T.; Cruciani, S.; Maradei, F.; Feliziani, M.: Magnetic shielding design of wireless power transfer systems, in *Proc. of 2015 IEEE Applied Computational Electromagnetics (ACES), Williamsburg, VA, USA*, March 22–26, 2015, 1–2.

[13] Choi, S.Y.; Gu, B.W.; Lee, S.W.; Lee, W.Y.; Huh, J.; Rim, C.T.: Generalized active EMF cancel methods for wireless electric vehicles. IEEE Trans. Power Electron., **29** (11) (2014), 5770–5783.

[14] ICNIRP Guidelines: Guidelines for limiting exposure to time-varying electric and magnetic fields (1 Hz - 100 kHz). Health Phys. **99** (6) (2010), 818–836.

[15] IEC 61980-1: Electric vehicle wireless power transfer (WPT) systems – Part 1: General requirements, 2015.

[16] Chan, C.C.; Jian, L.; Tu, D.: Smart charging of electric vehicles – integration of energy and information. IET Electrical Syst. Transportation, **4** (4) (2014), 89–96.

[17] SAE TIR J2954: Wireless power transfer for light-duty plug-in/electric vehicles and alignment methodology.

[18] Buccella, C.; Feliziani, M.; Fuina, V.; ELF magnetic field mitigation by active shielding. IEEE Int. Symp. Ind. Electron., **3**, (2002), 994–998.

[19] Caruso, C.; Feliziani, M.; Maradei, F.: ELF magnetic field produced by the ac electrification in a railway carriage, in P. Stavroulakis (Ed.), Biological Effects of Electromagnetic Fields, Springer Verlag, Berlin, Germany, 2003, 994–998.

[20] Schulz, R.B.; Plantz, V.C.; Brush, D.R.: Shielding theory and practice. IEEE Trans. Electromagn. Compat., **30** (3) (1988), 187–201.

[21] Campi, T.; Cruciani, S.; Maradei, F.; Feliziani, M.: Near-field reduction in a wireless power transfer system using LCC compensation. IEEE Trans. Electromag. Compat., **59** (2), 2017, 686–694.

[22] Feliziani, M. et al.; Robust LCC compensation in wireless power transfer with variable coupling factor due to coil misalignment, in *Proc. of 2015 IEEE 15th Int. Conf. on Environment and Electrical Engineering (EEEIC)*, Rome, Italy, June 10–13, 2015, 1181–1186.

[23] Campi, T.; Cruciani, S.; Maradei, F.; Feliziani, M.: Conducted emission of wireless power transfer charging system in electric vehicle, in *2017 IEEE International Symposium on Electromagnetic Compatibility & Signal/Power Integrity (EMCSI)*, Aug. 7–11, Washington DC, USA, 2017, 619–622.